RESEARCH ON THE CONTROL SYSTEM OF MOBILE STRAW COMPACTION MOLDING MACHINE BASED ON PSO-ELM-GPC MODEL
/
基于 PSO-ELM-GPC 模型的移动式秸秆致密成型机控制系统研究

Huiying CAI *[1]; Yunzhi LI [1]; Fangzhen LI [1]
[1] School of Computer Science and Technology, Shandong University of Finance and Economics, Jinan/ China
Tel: +86-18640598736; E-mail: caihuiying323@163.com

ABSTRACT

To address the issue of mutual influence and coupling between the main shaft speed and feeding amount of the mobile straw compaction molding machine, which is beneficial for the intelligent operation of the compaction molding, this paper designs a PSO-ELM-GPC control model. This model integrates Particle Swarm Optimization (PSO) algorithm, Extreme Learning Machine (ELM), and Generalized Predictive Control (GPC). It uses the ELM optimized by PSO to predict the output of the main shaft speed and feeding amount, and adjusts the input of the GPC controller based on the deviation weight adjustment unit. Field simulation experiments show that the maximum dynamic deviation of the speed is 1.72%, and the deviation from the target value is 1.52%. The maximum dynamic deviation of the feeding amount is 1.22%, and the deviation from the target value is 1.42%. The PSO-ELM-GPC model designed in this paper can promptly correct the uncertainties in speed and feeding amount control caused by disturbances.

摘要

为解决移动式秸秆致密成型机主轴转速与喂入量相互影响相互耦合的问题，以利于致密成型机智能化作业，本文设计了 PSO-ELM-GPC 控制模型，集粒子群优化、极限状态机、广义预测控制于一体，采用粒子群优化后的极限状态机对主轴转速与喂入量做出预测输出，依据偏差权重调整单元对 GPC 控制器输入量做出调节。场地模拟试验表明，转速最大动态偏差为 1.72%，与目标值的偏差为 1.52%；喂入量最大动态偏差为 1.22%，与目标值的偏差为 1.42%。本文设计的 PSO-ELM-GPC 模型可及时校正干扰引起的转速与喂入量控制引起的不确定问题。

INTRODUCTION

China has abundant straw resources, with a total straw volume reaching 8.56×10^8 tons in 2023. Biomass pellets made from corn straw extrusion are a low-carbon and clean energy source, which is of great significance for building an environmentally friendly society and promoting rural revitalization (*Gheorghe et al., 2024*). Mobile compaction molding machines integrate straw collection, crushing, dust removal, and pellet production in the field, which can greatly reduce production and labor costs, and have become an important way to promote the comprehensive utilization of straw. However, there is a coupling issue between the straw feeding amount and the main shaft speed during the operation of mobile straw compaction molding machines. The mismatch and lack of coordination between the feeding amount and main shaft speed affect the efficiency of the compaction molding machine in field operations.

To improve the work efficiency of mobile compaction molding machines, scholars at home and abroad have conducted extensive research. By analyzing the straw compacting process, the main factors affecting work efficiency are identified as straw feeding amount, main shaft speed, and straw moisture content. *Rostami et al., (2022),* studied the mutual influence of combine forward speed, reel index, field capacity, and pre harvest loss of a new designed combine harvester. *Abbas, (2019),* investigated the combine harvester speed, threshing cylinder speed and concave clearance on threshing losses and some related parameters during harvesting and suggested a strong correlation relationship between these parameters.

---

[1] *Huiying Cai, Associate Prof.; Yunzhi Li, Associate Prof.*

Choi et al., (2018), fabricated and evaluated the performance of the grain flow sensor suitable to the mid-sized full-feed type combine for rice, soybean, and barley, indirectly indicated the relationship between grain flow rate and production efficiency. *Chansrakoo et al., (2018)*, investigated the influence of grain moisture content, rotor speed, and feed rate to the performance of a short axial-flow soybean unit. *Birania et al. (2021) studied the relationship between feed rate and output of the small-scale pellet-making machine and specified that a satisfactory output could be obtained at a certain feed rate.* *Wang Wei et al., (2024)* established a work speed control model for the compaction molding machine based on a stable feeding amount on mobile compaction molding machines. Although the above research has made some progress, the coupling problem between feed rate and pressure roller spindle speed has not been considered. The coupling issue between the feeding amount and speed requires further in-depth research to further improve the work efficiency of the compaction molding machine.

Reasonable feeding amount and main shaft speed determine the work efficiency of the compaction molding machine. If the feeding amount is too large and the main shaft speed of the roller is low, the granulating device of the compaction molding machine is prone to clogging. If the feeding amount is too small and the main shaft speed is too high, the energy consumption is high, which affects the work efficiency of the compaction molding machine. To solve the coupling characteristics between feed rate and spindle speed and improve the efficiency of the molding machine, this paper takes the 560XC straw collection compaction molding machine designed by Liaoning Ningyue Agricultural Machinery Equipment Co., Ltd. as the research object. In view of the coupling problem between feeding amount and main shaft speed, a new decoupling control method is established based on POS and ELM, using GPC technology. The effectiveness and correctness of this algorithm are verified through field harvest tests and field trials.

MATERIALS AND METHODS
Structure and working principle of the control system
Overall structure

The control system of the mobile straw compaction molding machine consists of a hydraulic control device, a speed sensor, and a pellet molding device, as shown in Fig. 1. During operation, the mobile straw compaction molding machine is crushed by the front picking device, then thrown into the spiral conveyor, crushed for the second time, and conveyed through the feeding tube, and finally, the straw strands are squeezed and formed inside the forming device. The working process is shown in Fig. 2. The main shaft speed of the molding device is controlled by the hydraulic device, with the STM32F407 as the main microcontroller. The speed sensor gives a feedback to the main shaft speed. The driving speed determines the straw feeding amount.

Fig. 1 - Diagram of the straw compaction molding machine
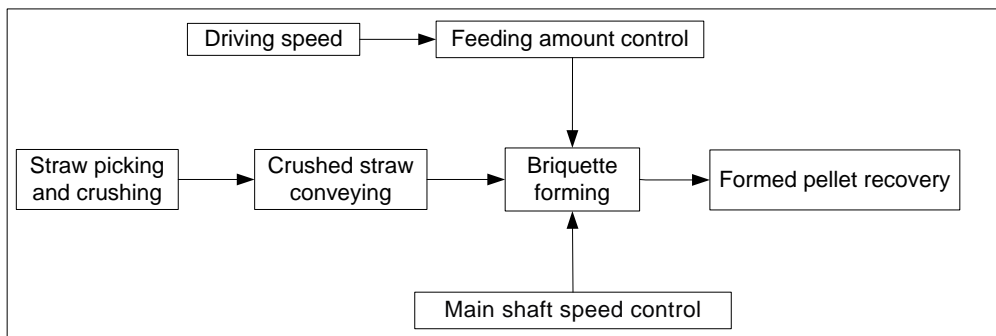*1 – Hydraulic control device; 2 – Speed Sensor; 3 – Pellet forming device; 4 – Biomass pellet*

Fig. 2 - Flow diagram for straw pelletizing process of the molding machine

Composition and Working Principle of the Control System

The control system of the mobile straw compaction molding machine consists of an industrial computer, microcontroller control, driving hydraulic transmission, granulation main shaft hydraulic transmission, granulation main shaft speed sensor, and driving speed sensor. The principle of the control system is shown in Fig. 3. The microcontroller's D/A output terminal 1 controls the driving hydraulic transmission mechanism, with the driving speed feedback by the driving speed sensor. D/A output terminal 2 controls the granulation main shaft hydraulic transmission mechanism, with the main shaft speed feedback by the granulation main shaft speed sensor. The industrial computer displays all control and monitoring information.
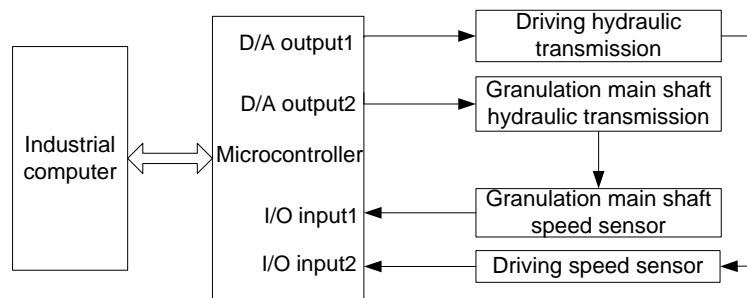

Fig. 3 - Structure of the molding machine control system

PSO-ELM Forecasting Method
ELM (Extreme Learning Machine)

ELM is intelligent algorithm that used widely in agriculture (*John, 2021*). It is a feedforward neural network with a single hidden layer, as shown in Fig. 4. During training, the input layer weight matrix and the hidden layer matrix of the ELM are randomly selected. By simply providing the number of neurons in the hidden layer, the global optimal target value can be obtained. It has the advantages of fast training speed and strong generalization ability.
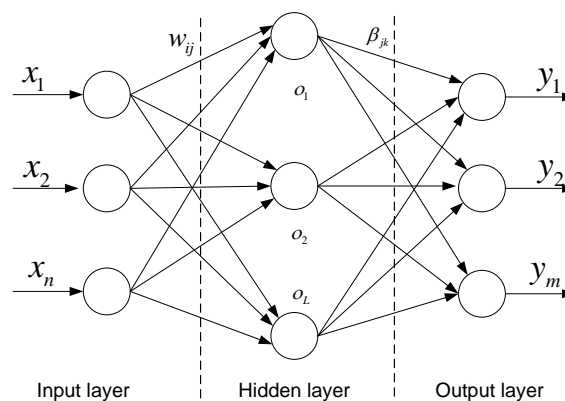

Fig. 4 - Structure of the molding machine control system

The input matrix of *n* neurons in the input layer is denoted as $X = [x_{i1}, x_{i2}, ..., x_{in}]^T$. The output matrix is denoted as $Y = [y_{i1}, y_{i2}, ..., y_{im}]^T$. The M model of the hidden layer activation function $g(x)$ is denoted as:

$$\sum_{i=1}^{L} \beta_{jk} g(\omega_{ij} \cdot x_{ij} + b_i) = y_i, j = 1, 2, \cdots, N \tag{1}$$

where:

β_{jk} is the connection weight between the hidden layer and the output layer neurons; ω_{ij} is the connection weight between the input layer and the hidden layer neurons; b_i is the threshold of the *i*-th neuron in the hidden layer; y_i is the actual output value.

The hidden layer output matrix H can be expressed as:

$$H = \begin{pmatrix} g(w_1 \cdot x_1 + b_1) & \cdots & g(w_L \cdot x_1 + b_L) \\ \vdots & \ddots & \vdots \\ g(w_1 \cdot x_N + b_1) & \cdots & g(w_L \cdot x_N + b_L) \end{pmatrix} \tag{2}$$

where:

$w_i = [\omega_{i1}, \omega_{i2}, ..., \omega_{iN}]^T$, represent the weight vector.

The network output is denoted as:

$$H\beta = Y' \tag{3}$$

The weight matrix denoted as $w = [\omega_1, \omega_2, ..., \omega_N]^T$, threshold vector $b = [b_1, b_2, ..., b_L]^T$. When $L = N$, the prediction result is independent of the size of w and b. The network output can approximate the training samples. That is:

$$\sum_{j=1}^{N} \left\| y_j - t_j \right\| = 0 \tag{4}$$

$$\min \left\| H\beta - T \right\| < \varepsilon \tag{5}$$

where:

T is the desired network output; ε is the network output error, when N is sufficiently large, $\varepsilon < 0$.

The connection weight value calculated by the minimum norm least squares criterion is:

$$\beta = H^+T \tag{6}$$

where:

H^+ is the pseudo-inverse of H.

Optimization for ELM by PSO

Due to the strong nonlinear characteristics between the main shaft speed and feeding amount of the compaction molding machine, the ELM is used for its simple structure, fast training speed, and strong nonlinear characterization ability to predict the main shaft speed and feeding amount. However, the random initialization of w and b in ELM can lead to the generation of useless neurons during operation, which affects the prediction accuracy. To reduce the error, this paper adopts the PSO (Particle Swarm Optimization) algorithm (*Naveed, 2024; Chen, 2023*) to optimize w and b, establishing a PSO-ELM (Swarm Optimization Algorithm-Extreme Learning Machine) forecasting model.

A population consisting of *n* particles is represented as $X = [x_1, x_2, \ldots x_n]$, which searches for the optimal value within this space. The parameters of particle *i* consists: velocity $V_i = [v_{i1}, v_{i2}, \ldots, v_{iD}]^T$, position $X_i = [x_{i1}, x_{i2}, \ldots x_{iD}]^T$, individual extreme value $P_i = [P_{i1}, P_{i2}, \ldots, P_{iD}]^T$; global extreme value $P_g = [P_{g1}, P_{g2}, \ldots, P_{gD}]^T$.

During the iteration process, the particles continuously search for the optimal velocity and position based on P_i and P_g, updating as:

$$V_{id}^{k+1} = \omega V_{id}^k + c_1 r_1 (P_{id}^k - X_{id}^k) + c_2 r_2 (P_{gd}^k - X_{id}^k) \tag{7}$$

$$X_{id}^{k+1} = X_{id}^k + V_{id}^{k+1} \tag{8}$$

where:

w is the inertia weight; $i = 1, 2, \ldots, n$; $d = 1, 2, \ldots, D$; k is the current iteration number; c_1, c_2 are acceleration factors to be negative constants; r_1, r_2 are random numbers distributed between [0, 1]. The velocity and position are continuously updated according to the particle fitness value to obtain the optimal solution.

Using the PSO-ELM method to predict the main shaft speed and feeding amount of the compaction molding machine, the model's w and b are optimized as particles in PSO to improve their accuracy, as shown in the Fig. 5.
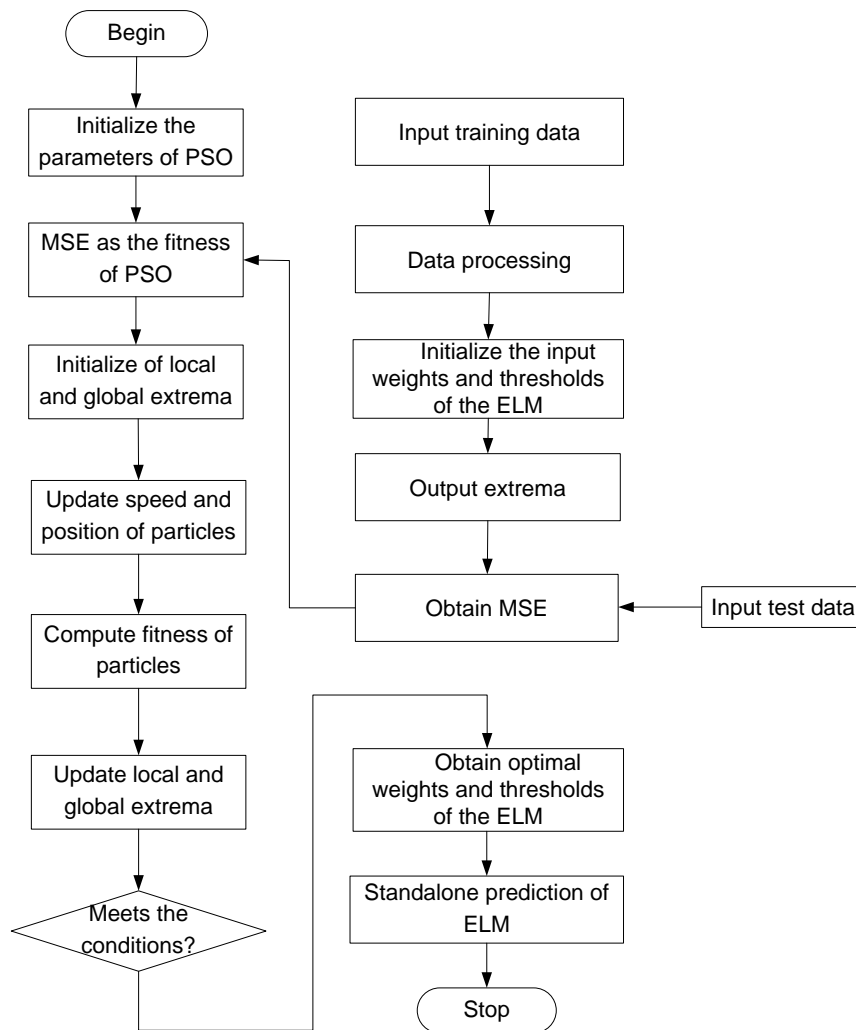
Fig. 5 - Flowchart of PSO-ELM model

RESULTS
Generalized Predictive Decoupling Control Based on PSO-ELM Model
Generalized Predictive Controller Design

The CARIMA (Controlled Autoregressive Integrated Moving Average) model (*Ma, 2022*) expression is denoted as:

$$A\left(z^{-1}\right)y\left(k\right)=B\left(z^{-1}\right)u\left(k-1\right)+\frac{C\left(z^{-1}\right)\varepsilon\left(k\right)}{\Delta} \tag{9}$$

where:

$$A\left(z^{-1}\right)=1+a_1z^{-1}+a^2z^{-2}+\cdots+a_nz^{-n}$$
$$B\left(q^{-1}\right)=b_0+b_1z^{-1}+b^2z^{-2}+\cdots+b_mz^{-m}$$

During field operations of the compaction molding machine, the environment is complex, which can lead to model mismatch and affect control accuracy. By introducing a performance function that minimizes multi-step prediction and control increments, a control sequence for future moments can be obtained, enhancing the system's stability. The performance index function is expressed as:

$$J_1\left(k\right)=E[\sum_{j=1}^{P}\left(y_M\left(k+j\right)-y_r\left(k+j\right)\right)^2+\sum_{j=0}^{L-1}\lambda\left(\Delta u\left(k+j\right)\right)^2] \tag{10}$$

where: $E[\cdot]$ is the variance function; L is the control horizon; λ is the control increment weighting coefficient; $y_M(k+j)$ is the predicted value at time $k+j$; P is the control time domain; $\Delta u(k+j)$ is the control change between adjacent sampling times.

After introducing and solving the Diophantine equation (*Fernandez B., 2018*), the predicted model's output value at time *k + j* is obtained as:

$$Y = G\Delta U + H\Delta \tilde{u} + F\tilde{y}(k) \tag{11}$$

where:

$$Y = \left[y(k+1) \cdots y(k+N) \right]^T$$

$$\Delta U = \left[\Delta u(k) \cdots \Delta u(k+M-1) \right]^T$$

$$\Delta u = \left[\Delta u(k-1) \cdots \Delta u(k-n_b) \right]^T$$

$$\tilde{y}(k) = \left[y(k) \cdots y(k-n_a) \right]^T$$

$$G = \begin{bmatrix} g_1 & & 0 \\ \vdots & \ddots & \\ g_M & \cdots & g_1 \\ \vdots & \ddots & \vdots \\ g_N & \cdots & g_{N-M+1} \end{bmatrix}$$

$$H = \begin{bmatrix} g_{1,1} & g_{1,2} & \cdots & g_{1,n_b} \\ g_{2,2} & g_{2,3} & \cdots & g_{2,n_{b+1}} \\ \vdots & & \ddots & \vdots \\ g_{N,N} & \cdots & \cdots & g_{N,N+n_b-1} \end{bmatrix}$$

$$F = \begin{bmatrix} f_{1,0} & f_{1,2} & \cdots & f_{1,n_a} \\ f_{2,0} & \ddots & & \vdots \\ \vdots & & \ddots & \vdots \\ f_{N,0} & \cdots & \cdots & f_{N,n_a} \end{bmatrix}$$

To ensure a smooth transition of the compaction molding machine's main shaft speed to the set value *w*, the reference trajectory is in the form of a first-order smoothing model, which is expressed as:

$$\begin{cases} y_r(t) = y(t) \\ y_r(t+j) = ay_r(t+j-1) + (1-a)w \end{cases} \tag{12}$$

where:

a is the softening coefficient, $a \in [0, 1]$; $y_r(t)$ is the desired output value of the speed; $y(t)$ is the actual output value of the speed; *w* is the set value of the speed.

Substituting Equation (11) into Equation (10), and taking the derivative of the performance index function *J* with respect to *t*, the optimal solution expression for $J_1(k)$ can be obtained as:

$$u(t) = u(t-1) + \left(G^T G + \lambda I\right)^{-1} G^T \left(W - H\Delta u - F\, y(k)\right) \tag{13}$$

where: *I* and *W* are the identity matrix with different size.

Generalized Predictive Control of the Molding Machine Based on the PSO-ELM Model

The process control structure diagram of predictive decoupling control method based on the PSO-ELM model for the main shaft speed and feeding amount of the molding machine is shown in Fig. 6.

Monitoring the output values of the main shaft speed and the feeding amount entering the compaction molding machine, denoted as y = {y₁, y₂}, calculate the deviation e = {e₁, e₂} of the output values from the reference values ω = {ω_1, ω_2}, and use this deviation as the input of the decoupling controller. The decoupling controller adaptively adjusts its strategy based on the deviation to improve decoupling performance. After optimization by the controller, the control amount u = {u₁, u₂} adjusts the main shaft speed and feeding amount, thereby improving the production efficiency of the biomass pellets produced by the compaction molding machine.
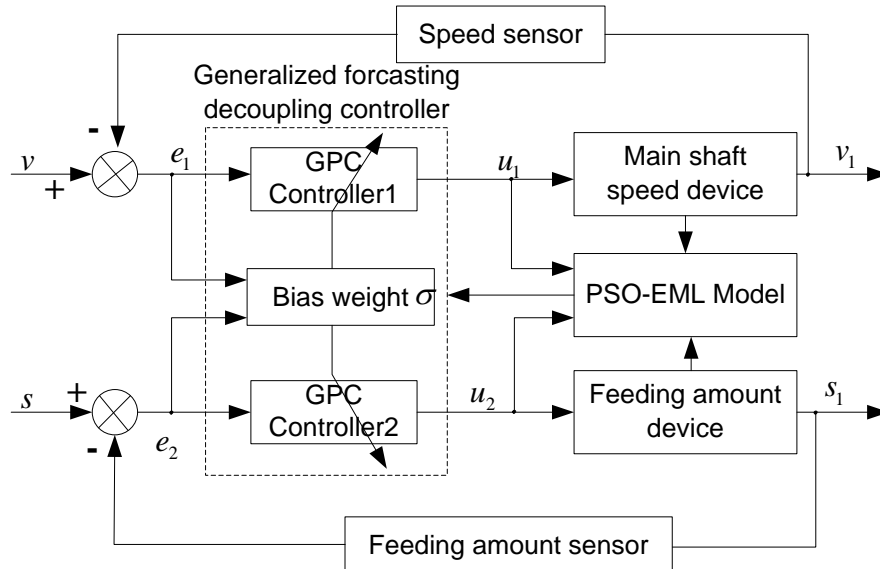

Fig. 6 - Process control structure of the molding machine based on the PSO-ELM model

In the decoupling controller, the deviation weight is decoupled based on the deviation between the predicted output value and the reference trajectory. When a certain deviation occurs between the predicted output value y of the main shaft speed loop and the reference value ω, the deviation weight $\alpha_i(k+t)$ of the feeding amount loop is adjusted to increase the output error weight of the feed rate loop, thereby increasing the control increment at the next moment and reducing the impact of the output change of the main shaft speed loop on the feeding amount loop, achieving the purpose of suppressing loop coupling. Similarly, the coupling effect of feed rate on speed can be eliminated according to this principle. The calculation formula for $\alpha_i(k+t)$ is expressed as:

$$\alpha_i(k+t) = \alpha_i(0) + \sum_{p=1}^{2}\theta_{ip}\left[\hat{y}_p(k+p) - \omega_p(k+t)\right]^2 \tag{14}$$

where: $\alpha_i(0)$ is the initial value of $\alpha_i(k+t)$; θ_{ip} is the amplification coefficient.

Transfer function models for speed control and feed rate control are established through experiments. They are expressed as equation (15) and equation (16) respectively.

$$G_1(s) = \frac{8.34\times10^{-3}}{\left(\dfrac{s^2}{495.7^2} + \dfrac{3.6}{495.7}s + 1\right)} \tag{15}$$

$$G_2(s) = \frac{21932.4}{s(0.0034s+1)\left(\dfrac{s^2}{5.4^2} + \dfrac{4}{27}s + 1\right)} \tag{16}$$

Experiments and analysis

To verify the effectiveness of the generalized predictive decoupling control system proposed in this paper, a simulation harvest test was conducted on March 20, 2024, at Liaoning Ningyue Agricultural Machinery Equipment Co., Ltd. in Heishan County, Liaoning Province.

A 560XC straw compaction molding machine was selected for the experiments. A rectangular straw bed measuring 60 meters in length and 2 meters in width was laid out in the experiment site, as shown in Fig.7.

The main test equipment included an industrial computer (ZPC150-T112 model), a feed rate sensor (NY-DF01), and a speed sensor (SC12-20K). The industrial computer processor was Intel(R) Core(TM) i5-3337U CPU@1.8Hz, with a 64-bit Windows 10 operating system and 16GB of memory.

Fig. 7 - Granulation experiment

The performance comparison of the field granulation experiment controllers is shown in Table 1. In the PSO-ELM-GPC controller, the adjustment time of the speed of the main shaft is shortened by 8.1% and 32.7% compared to the GPC and PID controllers (*Savaniu et al., 2023; Hajiahmadi et al., 2024*), with the smallest speed overshoot of 8.42%. The adjustment time of the feed rate is shortened by 19.9% and 34.7% compared to the GPC and PID controllers, with the smallest feed rate overshoot of 8.97%.

The speed error curve and the feed rate error change curve are shown in Fig. 8 and Fig. 9, respectively. Under the control of the PSO-ELM-GPC model, the maximum dynamic deviation of the speed is 1.72%, with a deviation of 1.52% from the target value; the maximum dynamic deviation of the feed rate is 1.22%, with a deviation of 1.42% from the target value.

Table 1

Controller performance parameters

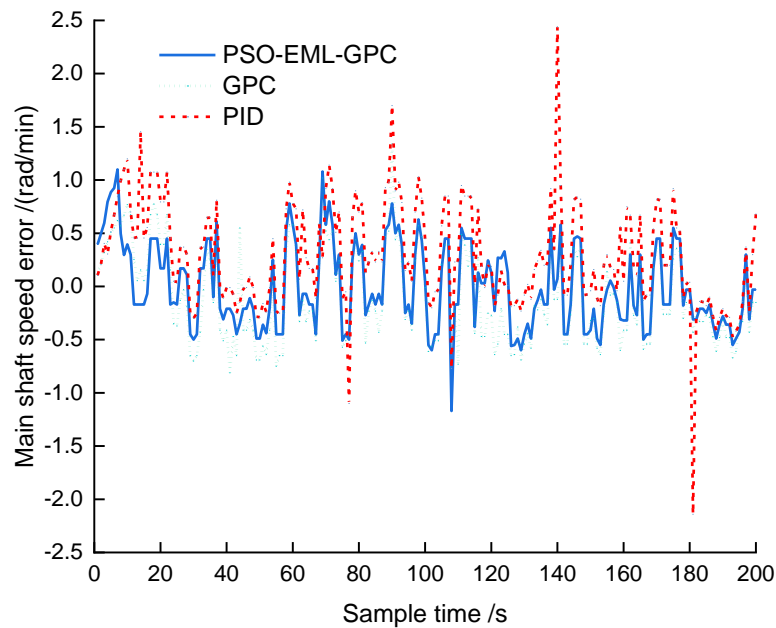| Control algorithm	main shaft speed		feeding amount	
	Regulation	Overshoot	Regulation	Overshoot
	[s]	[%]	[s]	[%]
PID	11.62	10.35	14.34	12.46
GPC	8.51	9.32	11.69	10.82
PSO-ELM-GPC	7.82	8.42	9.36	8.97

Fig. 8 - Error curve of main shaft speed
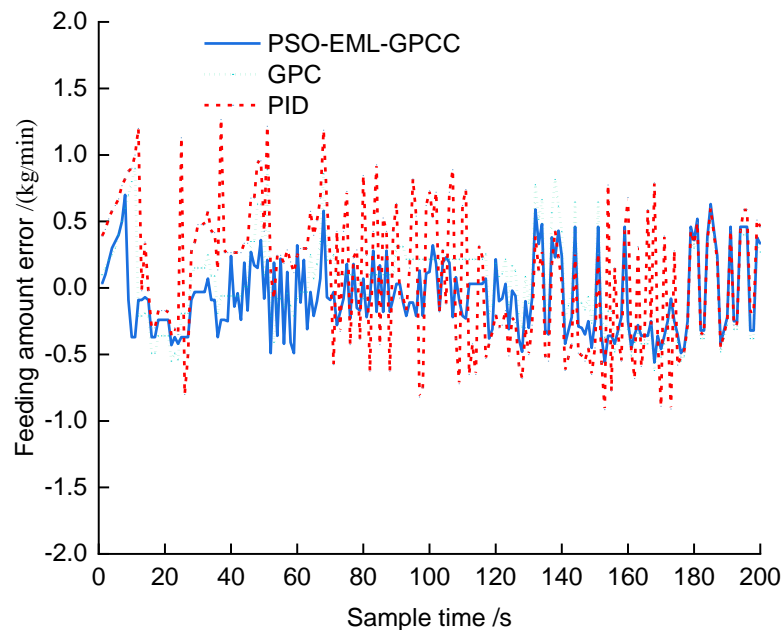

Fig. 9 - Error curve of feeding amount

CONCLUSIONS

(1) A PSO-ELM-GPC decoupling controller model was designed to eliminate the mutual influence between the main shaft speed and feeding amount of the mobile densification molding machine.

(2) In the PSO-ELM-GPC decoupling controller model, PSO was used to optimize the parameters in ELM, which predicts the main shaft speed and feeding amount. The input deviation weight adjustment unit adjusts the input of the GPC controller.

(3) Field simulation experiments showed that the maximum dynamic deviation of the speed was 1.72%, with a deviation of 1.52% from the target value; the maximum dynamic deviation of the feed rate was 1.22%, with a deviation of 1.42% from the target value. The PSO-ELM-GPC model designed in this paper can meet the on-site operation requirements of the mobile straw compaction molding machine.

ACKNOWLEDGEMENT

REFERENCES

[1]   Abbas, A. A. (2019). The effect of combine harvester speed, threshing cylinder speed and concave clearance on threshing losses of rice crop. *Journal of Engineering and Applied Sciences*. http://10.36478/jeasci.2019.9959.9965

[2]   Abdeen, M. A., Xie, G., Salem, A. E., Fu, J., & Zhang, G. (2022). Longitudinal axial flow rice thresher feeding rate monitoring based on force sensing resistors. *Scientific Reports*, 12(1), 1369. https://www.nature.com/articles/s41598-021-04675-w

[3]   Birania, S., Yadvika, Garg, M. K., Gupta, R., Kumar, R., & Kumar, N. (2021). Development and performance evaluation of biomass pellet machine for on-farm sustainable management and valorization of paddy straw. *Environmental Engineering and Management Journal*, 20(12), 2013-2023. http://10.30638/eemj.2021.187

[4]   Chansrakoo, W., Chuan-Udom, S. (2018). Factors of operation affecting performance of a short axial-flow soybean threshing unit. *Engineering Journal*, 22(4), 109-120. http://10.4186/ej.2018.22.4.109

[5]   Chen, L. I. (2023). Path planning of fruit and vegetable picking robots based on improved A* algorithm and particle swarm optimization algorithm. *INMATEH-Agricultural Engineering*, 71(3). https://doi-org-s.libyc.nudt.edu.cn:443/10.35633/inmateh-71-41

[6]   Choi, M. C., Lee, K. H., Jang, B. E., Kim, Y. J., & Kim, S. K. (2018). Grain flow rate sensing for a 55 kW full-feed type multi-purpose combine. *International Journal of Agricultural and Biological Engineering*, 11(5), 206-210. http://10.25165/j.ijabe.20181105.2686

[7]   Fernandez, B., Herrera, P. J., & Cerrada, J. A. (2018). Self-tuning regulator for a tractor with varying speed and hitch forces. *Computers and Electronics in agriculture*, 145, 282-288. https://doi.org/10.1016/j.compag.2017.12.027

[8]   Gheorghe, D., & Neacsu, A. (2024). The influence of additives upon the energetic parameters and physicochemical properties of environmentally friendly biomass pellets. *Journal of the Mexican Chemical Society*, 438-454. https://doi.org/10.29356/jmcs.v68i3.2032

[9]   Hajiahmadi, F., Jafari, M., & Reyhanoglu, M. (2024). Machine learning-based control of autonomous vehicles for solar panel cleaning systems in agricultural Solar Farms. *AgriEngineering*, 6(2), 1417-1435. https://doi.org/10.3390/agriengineering6020081

[10]   John, S., & Rose, A. L. (2021). Machine learning techniques in plant disease detection and classification-a state of the art. *INMATEH-Agricultural Engineering*, 65(3), 362-372. https://doi.org/10.35633/inmateh-65-38

[11]   Ma, C., Li, X., Xiang, G., & Dian, S. (2022). A TS Fuzzy quaternion-value neural network-based data-driven generalized predictive control scheme for mecanum mobile robot. *Processes*, 10(10), 1964. https://doi.org/10.3390/pr10101964

[12]   Naveed, M. H., Gul, J., Khan, M. N. A., Naqvi, S. R., Štěpanec, L., & Ali, I. (2024). Torrefied biomass quality prediction and optimization using machine learning algorithms. *Chemical Engineering Journal Advances*, 19, 100620. https://doi.org/10.1016/j.ceja.2024.100620

[13]   Rostami, M. A., Shaker, M., Bakhtiari, M. R. (2022). Economic and technical feasibility of replacing conventional combines with a new straw crusher combine. *Agricultural Engineering International: CIGR Journal*, 24(3), 93-102.

[14]   Savaniu, I.M., Chiriță, A.P., Popovici, I.A., Tonciu, O., Culcea, M., Neagu, A., & Stefan, V. (2023). Optimizing and integrating electromechanical actuators in agricultural excavator booms for enhanced efficiency and battery longevity. *INMATEH - Agricultural Engineering*, 71(3), 335-344. http://10.35633/inmateh-71-29

[15]   Wang. W., Ji, D., Gong, Y. J., Bai, X. W., Li, N., & Li H. Y. (2024). Spindle speed control method of straw picking compactor (基于 GPC-ILC 的秸秆捡拾致密成型机主轴转速控制方法研究). *Transactions of the Chinese Society of Agricultural Machinery*, 55(4), 83-90. http://10.6041/j.issn.1000-1298.2024.04.008